

# Power spectrum of many impurities in a $d$ -wave superconductor

Lingyin Zhu<sup>1</sup>, W. A. Atkinson<sup>2</sup>, and P. J. Hirschfeld<sup>1</sup>

<sup>1</sup>*Department of Physics, University of Florida, Gainesville FL 32611*

<sup>2</sup>*Department of Physics, Southern Illinois University, Carbondale IL 62901-4401*

(Dated: November 4, 2018)

Recently the structure of the measured local density of states power spectrum of a small area of the  $\text{Bi}_2\text{Sr}_2\text{CaCu}_2\text{O}_8$  (BSCCO) surface has been interpreted in terms of peaks at an “octet” of scattering wave vectors determined assuming weak, noninterfering scattering centers. Using analytical arguments and numerical solutions of the Bogoliubov-de Gennes equations, we discuss how the interference between many impurities in a  $d$ -wave superconductor alters this scenario. We propose that the peaks observed in the power spectrum are not the features identified in the simpler analyses, but rather “background” structures which disperse along with the octet vectors. We further consider how our results constrain the form of the actual disorder potential found in this material.

In the past few years, high-resolution scanning tunneling microscopy (STM) experiments on the cuprate superconductor BSCCO [1, 2, 3, 4, 5, 6, 7, 8, 9, 10, 11] have obtained local information on electronic structure for the first time. The first great success of this technique was the observation of resonant defect states at low temperatures in the superconducting state[1, 2, 3], confirming early proposals that such states should be reflected in the local density of states (LDOS) of  $d$ -wave superconductors[12, 13]. Subsequent experiments revealed the existence of nanoscale inhomogeneities[4, 5, 6, 7] which are currently the subject of debate, being attributed either to interaction-driven effects such as stripe-formation[8, 9] or to Friedel oscillations of weakly-interacting quasiparticles[5, 6]. At the heart of this debate lies the important question of whether, and if so in what ranges of doping, conventional BCS-like theories describe the ground state and low energy excitations of BSCCO. Recently it has been pointed out that, in inhomogeneous systems, the Fourier transform of the LDOS (FTDOS) contains information not only about the disorder potential, but about the kinematics of the associated pure system. That this must be so at some level is clear from the original one-impurity problem solved by Friedel[14]: a charge inserted in an electron gas gives rise to LDOS oscillations which vary at large distances as  $\sim \cos 2k_F r/r^3$ , so the wavelength of the LDOS “ripples” caused by a single impurity gives the Fermi wave vector directly. A somewhat more sophisticated version of this argument,[10, 15, 16, 17, 18] still assuming scattering from a single or few impurities and noninteracting quasiparticles, suggested that the peaks in the FTDOS are due to scattering of quasiparticles by a weak disorder potential. In this case favored momentum transfers correspond to vectors  $\mathbf{q}$  connecting two tips of quasiparticle constant energy contours which maximize the joint density of states (JDOS). This interpretation has been applied to recent experiments[11] which claim to map out a Fermi surface in agreement with angle-resolved photoemission (ARPES). In contrast to this, Howald et al.[8, 9] identify nondispersing features in the FTDOS from their

experiments, which they suggest are indicative of static-stripe formation along the Cu-O bond directions.

In this Letter, we report on numerical studies of models of disordered superconducting BSCCO. Previous analyses of a single weak impurity[15, 16] agreed qualitatively with the simple JDOS analysis of Ref. [11] and successfully predicted the dispersion of the peak positions in the FTDOS. It has been since shown[19] that the sharp 1-impurity peaks survive in the many-impurity case if the potential is sufficiently weak. However, the ability to correctly predict the peak positions (which depend only on the quasiparticle band structure, and not the disorder potential) does not imply that the low-energy excitations are understood. A full microscopic understanding of the superconducting state requires an accurate description of the disorder potential in the BSCCO  $\text{CuO}_2$  planes. We will show that there are both qualitative and quantitative problems describing experiments which stem from the inadequacy of the weak-impurity model, and that the FTDOS spectrum of a realistic model comprising a dilute concentration of unitary scatterers, together with a smooth disorder potential, is required to fit experiment and has features not present in the simple JDOS analysis. Understanding these discrepancies will be crucial to extracting reliable information about the clean system, as well as the nature of the disorder potential.

*Many Impurities.* In this section, we discuss the differences between the single and many-impurity FTDOS for weak pointlike scatterers, and compare these spectra with experiment. We first imagine a random distribution of  $N_I$  pointlike impurities located at sites  $\mathbf{R}_i$  with  $i = 1 \dots N_I$ . The LDOS can be formally decomposed  $\rho(\mathbf{r}, \omega) = \rho_0(\omega) + \delta\rho(\mathbf{r}, \omega)$  where  $\rho_0$  is the DOS of the homogeneous superconductor, and  $\delta\rho$  is the local shift due to disorder given exactly by

$$\delta\rho(\mathbf{r}, \omega) = -\frac{1}{\pi} \text{Im} \sum_{i,j=1}^{N_I} \left[ \hat{G}^0(\mathbf{r} - \mathbf{R}_i) \hat{T}_{ij} \hat{G}^0(\mathbf{R}_j - \mathbf{r}) \right]_{11} \quad (1)$$

where the  $\omega$ -dependence is suppressed for clarity,  $\hat{T}(\omega)$  is the  $2N_I \times 2N_I$  many-impurity T-matrix (the factor of two

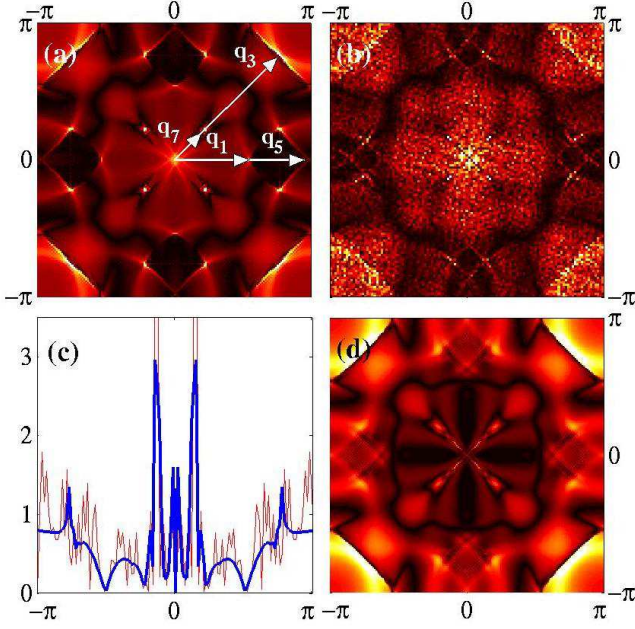


FIG. 1: FTDOS at  $\omega = 14$  meV for weak potential scatterers ( $V_0 = 0.67t_1$ ): (a) for one weak impurity, with a few important scattering wavevectors indicated; (b) for 0.15% weak scatterers. Cuts through the data of (a) (thick line) and (b) (thin line) along the (110) direction and scaled by  $1/\sqrt{N_I}$  are plotted vs.  $q_x$  in (c), while (d) shows the weak scattering response function  $\text{Im } \Lambda_3(\mathbf{q}, \omega)$ . Peaks at  $\mathbf{q} = 0$  are removed for clarity. In all figures, the  $x$  and  $y$  axes are aligned with the Cu-O bonds.

arises from spin),  $\hat{G}^0(\mathbf{r}, \omega)$  is the bare electron Green's function  $\hat{G}^0(\mathbf{r}, \omega) = \sum_{\mathbf{k}} \hat{G}^0(\mathbf{k}, \omega) \exp(i\mathbf{k} \cdot \mathbf{r})$ ,  $\hat{\cdot}$  refers to matrices in the Nambu-spinor formalism and  $[\dots]_{ij}$  are spinor indices. The T-matrix is expressed in terms of the 1-impurity T-matrix  $\hat{t}_i = [1 - \hat{V}_i \hat{G}^0(\mathbf{r} = 0)]^{-1} \hat{V}_i$  by

$$\hat{T}_{ij} = \hat{t}_i \delta_{i,j} + \sum_{m=1}^{N_I} \hat{t}_i [1 - \delta_{m,i}] \hat{G}^0(\mathbf{R}_i - \mathbf{R}_m) \hat{T}_{mj}, \quad (2)$$

where the impurity potential at  $\mathbf{R}_i$  is  $\hat{V}_i = V_0 \hat{\tau}_3$ , and  $\hat{\tau}_i$  are the Pauli matrices. For pure potential scatterers, the T-matrix can be decomposed into two Nambu components  $\hat{t} = t_0 e^{i\phi_0} \hat{\tau}_0 + t_3 e^{i\phi_3} \hat{\tau}_3$  with  $t_0$  and  $t_3$  real, and  $\phi_0$  and  $\phi_3$  the scattering phase shifts.

Throughout this work, we adopt the ARPES-derived tight-binding model of Norman[20] for the band structure, and assume nearest-neighbor  $d$ -wave pairing with order-parameter  $\Delta_{\mathbf{k}} = \Delta_0(\cos k_x - \cos k_y)$  and  $\Delta_0 = 0.16t_1 = 24$  meV where  $t_1 = 150$  meV is the nearest-neighbor hopping matrix element. We take, as representative, the weak scattering potential  $V_0 = 0.67t_1$ . We ignore the effects of tunneling matrix elements[22, 23], and assume that the STM probe measures the LDOS  $\rho(\mathbf{r}, \omega)$  directly (note that  $\mathbf{r}$  need not correspond to a site  $\mathbf{R}$  of the crystal lattice). The Fourier transform is

then  $\rho(\mathbf{q}, \omega) = \sum_{\mathbf{r} \in L \times L} e^{-i\mathbf{q} \cdot \mathbf{r}} \rho(\mathbf{r}, \omega)$ , where  $L \times L$  is a square set of  $L^2$  positions at which measurements are made, and  $\mathbf{q} = 2\pi(m, n)/L$  are vectors in the associated reciprocal lattice.

The FTDOS is shown at  $\omega = 14$  meV in Fig. 1 for (a) a single impurity[24] (b) a collection of  $N_I = 21$  (0.15%) weak scatterers on a  $120 \times 120$  lattice. Using the notation of Ref. [11], a few important peak positions which are predicted by the JDOS analysis are also shown in Fig. 1(a). To understand the relationship between Figs. 1(a) and (b), we consider Eq. (1) to leading order in  $\hat{t}_i$ :

$$\delta\rho(\mathbf{q}, \omega) \simeq -\frac{1}{\pi} \sum_{\alpha=0,3} t_{\alpha}(\mathbf{q}) \text{Im}[e^{i\phi_{\alpha}} \Lambda_{\alpha}(\mathbf{q}, \omega)] \quad (3)$$

where  $t_{\alpha}(\mathbf{q}) = t_{\alpha} \sum_i e^{-i\mathbf{q} \cdot \mathbf{R}_i}$  and  $\Lambda_{\alpha}(\mathbf{q}, \omega) = \sum_{\mathbf{k}} [\hat{G}^0(\mathbf{k}, \omega) \hat{\tau}_{\alpha} \hat{G}^0(\mathbf{k} + \mathbf{q}, \omega)]$ . Eq. (3) affords a clear separation between degrees of freedom associated with the disorder potential and those of the pure system, which is not possible if scattering processes of higher order in  $\hat{t}_i$  are important. Since  $t_{\alpha}(\mathbf{q})$  consists of a sum of  $N_I$  random phases, it becomes a random function of  $\mathbf{q}$  in the first Brillouin zone as  $N_I \rightarrow \infty$ . By contrast,  $\Lambda_{\alpha}(\mathbf{q}, \omega)$  is the response function of the clean system, is independent of the disorder potential, and determines the peak locations and widths in the FTDOS. As is evident in Fig. 1(c), JDOS peaks are *not broadened* or shifted by disorder; note in particular that the thin line representing the many-impurity case shows a sharp  $\mathbf{q}_7$  peak which is visible only as one or two bright pixels in Fig. 1(b).

In the limit of weak potentials, Eq. (3) reduces to the result of Capriotti et al[19],

$$\delta\rho(\mathbf{q}, \omega) \simeq -V(\mathbf{q}) \text{Im } \Lambda_3(\mathbf{q}, \omega) / \pi, \quad (4)$$

which is also valid for finite range  $V(\mathbf{r})$ . The effect of an extended potential can be understood with an example: if the single-impurity potential is  $V_0(\mathbf{r}) = v_0 \exp(-r^2/2r_0^2)$ , then  $V(\mathbf{q}) = 2\pi r_0^2 v_0 \exp(-q^2 r_0^2/2) \sum_i \exp(i\mathbf{q} \cdot \mathbf{R}_i)$ . Thus, for sufficiently weak scatterers, the  $q$ -space structure of  $\delta\rho(\mathbf{q}, \omega)$  is determined primarily by the band structure, but has an envelope which suppresses the FTDOS near the Brillouin zone edges, and is noisy because of randomness in the impurity positions. We remark that since  $\Lambda_3(\mathbf{q}, \omega)$  can be calculated from knowledge of the electronic structure of the pure system, Eq. (4) is, in principle, a useful tool for determining the scattering potential directly from experimental measurements of the LDOS. However, we caution the reader that Eq. (4) applies only to unphysically weak potentials. Figure 1(d) shows that even for the weak potential  $V_0 = 0.67t_1$ , not all peaks in the FTDOS (notably the central peak around  $q = 0$ ) are reproduced by Eq. (4).

While Eqs. (3) and (4) appear to suggest that the dispersing 1-impurity peaks are also present for many impurities, we can show from Eq. (3) that in the disorder average  $\langle |\delta\rho(\mathbf{q}, \omega)|^2 \rangle \sim N_I$  and  $\langle |\delta\rho(\mathbf{q}, \omega)|^4 \rangle - \langle |\delta\rho(\mathbf{q}, \omega)|^2 \rangle^2 \sim$



$N_I(N_I - 1)$ , implying that the noise is actually as large as the signal. As a consequence, the weak  $\mathbf{q}_1$  peaks present in Fig. 1(a) are lost in the noise in Fig. 1(b), and the broader background features are relatively enhanced. Thus, it appears that the peaks predicted by the JDOS analysis may not be robust when many impurities are present. This is particularly true when the effects of energy resolution  $\Delta\omega$  are considered. In Ref. [11],  $\Delta\omega \approx 2$  meV[27], and we use a complex energy  $\omega + i\gamma$  in our calculations which for  $\gamma = 0.015t_1 = 2.25$  meV yields a comparable resolution. We find that even for one impurity, FTDOS peaks are extremely sensitive to  $\gamma$ . All peaks are suppressed, *but not broadened*, as  $\gamma$  increases (this conclusion differs from Ref. [16]).

It is therefore difficult to understand, based on the weak impurity analysis, why experiments measure *broad* and well-defined  $\mathbf{q}_1$  and  $\mathbf{q}_7$  peaks of roughly equal weight. Furthermore, 1-impurity calculations such as in Fig. 1(c) find in addition to JDOS peaks a highly structured dispersive “background” structure, whereas in current interpretations of experiments all features are ascribed to JDOS peaks. Our calculations suggest that, because of noise, it may be easy to confuse dispersing background features and JDOS peaks in experiments. Very recently, it was pointed out in Ref. [21] that the scattering amplitude for processes involving  $\Lambda_0(\mathbf{q})$  is not sharply peaked at the “octet”  $\mathbf{q}_\alpha$ , but our analysis shows further that the predominant structures in the presence of noise are generally considerably shifted from the  $\mathbf{q}_\alpha$  positions, and may indeed be associated with off-shell processes.

*Realistic Disorder Models.* The weak-scattering pointlike disorder model is convenient for its simplicity, but does not predict FTDOS peak widths consistent with experiment. In addition, the relative weights of the features ascribed to the  $\mathbf{q}_\alpha$  (e.g., the nearly equal weight of  $\mathbf{q}_7$  and  $\mathbf{q}_1$ ) are not correctly predicted, particularly at low energies. In this section, we explore whether the measured FTDOS can be explained by a simple “realistic” disorder model. Two types of disorder, unitary defects and intrinsic nanoscale inhomogeneities are known to be present in nominally clean BSCCO. In the experiments of Ref. [11], a concentration of  $\approx 0.2\%$  unitary, pointlike native defects were observed, while in Refs. [4, 5, 6, 7, 8, 9] nanoscale inhomogeneities were observed with a typical size of  $\approx 2$  nm. In this work, we model the native defects as pointlike scatterers with an on-site potential  $V_0 = 30t_1$  which produces a local resonance centered at 0 meV (the concentration and strength of the unitary defects is thus fixed by experiment within the potential scattering model). The source of the nanoscale inhomogeneity is unknown, and we take the simplest ansatz, that it arises from a smooth random potential, probably originating from charge inhomogeneities in the BiO layers. For definiteness, we model the smooth potential as  $V(\mathbf{r}) = \sum_i V(i) \exp(-\tilde{r}_i/\lambda)/\tilde{r}_i$  and  $\tilde{r}_i = [(\mathbf{r} - \mathbf{R}_i)^2 + d_z^2]^{1/2}$ , where  $\mathbf{R}_i + \hat{\mathbf{z}}d_z$  are the defect locations,  $V(i)$  are the defect potentials and  $\lambda$  is a screening length. We take a bimodal distribution  $V(i) = \pm V$  so

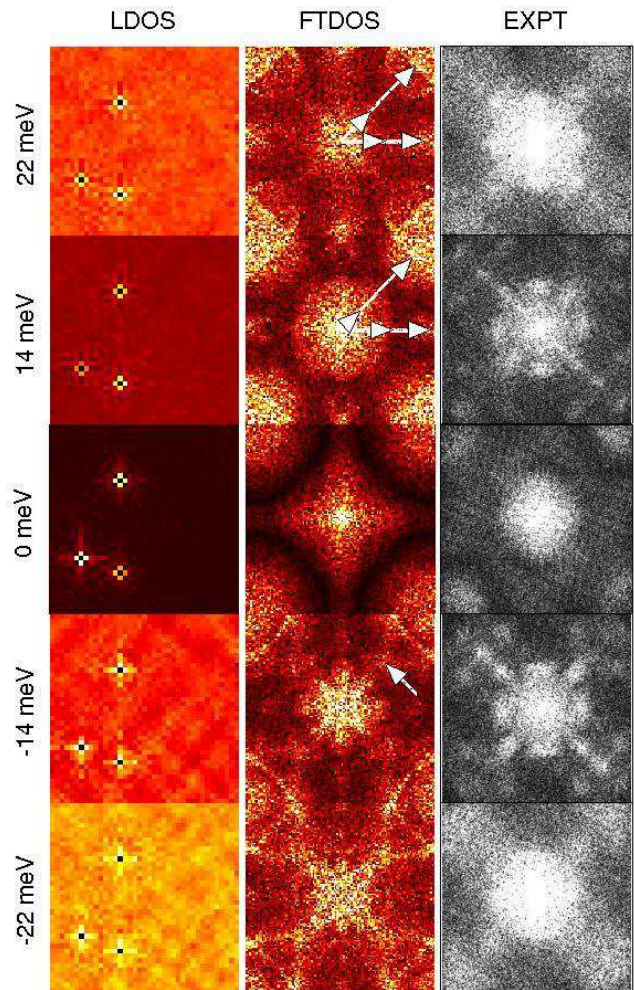


FIG. 2: Comparison of theory and experiment. Calculated LDOS and FTDOS are compared with experimental FTDOS (EXPT) at five energies. LDOS are shown for a  $40 \times 40$  subsection of the  $120 \times 120$  lattice. FTDOS are shown in the first Brillouin zone,  $-\pi/a \leq q_x, q_y \leq \pi/a$ . Theoretical calculations are for a mix of unitary pointlike and smooth potential scatterers. Scattering  $q$ -vectors are shown at 22 meV and 14 meV (negative energy vectors are the same). A broad background feature in the FTDOS is identified with an arrow at -14 meV.

that the smooth potential represents spatial fluctuations of the local potential about a mean which is determined by the doping level. Equation (2) applies to pointlike impurities only, so we use an implementation of the recursion method[25] to solve directly for the local Green’s function  $\hat{G}(\mathbf{r}, \mathbf{r}, \omega + i\gamma)$ , with  $\gamma = 2.25$  meV, of the inhomogeneous system. Our best-fit model consists of  $0.2\%$  unitary defects, and  $8\%$  smooth scattering centers with  $V = 2t_1$ ,  $d = 2a$  and  $\lambda = a$ .

We compare this mixed-impurity model with the experimental data of McElroy et al in Fig. 2. In both experiment and calculations, the local resonances are plainly evident in the LDOS for  $|\omega| \lesssim 15$  meV and, in our calcu-

lations, make the dominant contribution to the FTDOS. As with weak scatterers, the narrow JDOS peaks are swamped by noise, and suppressed by the finite energy resolution. However, unlike the weak scattering case, the  $\mathbf{q}_1$  and  $\mathbf{q}_5$  structures at 14 meV are relatively robust and remnants of the peaks can be seen. Excess weight relative to experiment in the Brillouin zone corners is probably due to finite potential range and sub-unit cell information obtained in experiment, both of which lead to a modulation of  $\delta\rho(\mathbf{q})$  which decays at large  $q$ [26].

For larger energies, the LDOS impurity resonances disappear in experiment but, because the electronic wavefunctions are excluded from the defect site, they remain clearly visible in our calculations. The discrepancy may arise because the STM tip height is adjusted to maintain a constant current at a fixed bias voltage (typically -150 meV in Ref. [11]), so that what is actually plotted is the LDOS relative to the average LDOS at that site. We will discuss the effect of tip-height adjustments elsewhere[26], and here we simply note that despite discrepancies, the Fourier transforms of the measured and predicted patterns are qualitatively similar. At energies  $|\omega| \gtrsim 15$  meV, the smooth random potential makes a significant contribution to the FTDOS.

The agreement between the calculated and experimental FTDOS is qualitatively good at low energies, although our calculations show more asymmetry between positive and negative energies, with the negative energy calculations fitting better, than in experiments. This is the result of the large, probably artificial, asymmetry of the model band, in which there is a van Hove singularity at  $\omega \approx -50$  meV that is not observed in tunneling experiments. As before, remnants of JDOS peaks (for example, the  $\mathbf{q}_1$  peak at -14 meV or the  $\mathbf{q}_5$  peak at 14 meV) are evident in the calculated FTDOS, but most of the structure comes from a set of broader dispersing features, which has been previously ignored. At -14 meV and -22 meV, we see that there are clear octet structures about the central peak, but that the dispersing “ $\mathbf{q}_7$ ” features [the arms along the  $(\pm\pi, \pm\pi)$  directions extending from the central peak] extend well beyond  $\mathbf{q}_7$ . In general, the background structures disperse qualitatively (growing or shrinking with  $|\omega|$ ) as one expects from the JDOS analysis.

Since the  $\mathbf{q}_7$  peak comes from intranodal scattering, it is a direct measure of the  $\mathbf{k}$ -dependence of the superconducting gap and scales with  $\sim 1/v_\Delta$ , where  $v_\Delta$  is the gap velocity at the nodes. The measured gap is not consistent with nearest-neighbor  $d$ -wave pairing—for example the experimental value at  $\omega = -14$  meV  $\mathbf{q}_7^{exp} \approx 0.6\pi/a$ [11] is nearly twice the value in our nearest-neighbor  $d$ -wave model—and the authors of Ref. [11] have been forced to introduce a significant subleading  $\cos 6\theta$

harmonic in their fit of the angular dependence of the gap on the Fermi surface. The additional harmonic is associated with pairing beyond near-neighbors, in contrast to ARPES results which suggest the gap is pure near-neighbor  $d$ -wave at optimal doping. Recognizing that the observed feature at roughly twice the true  $\mathbf{q}_7$  is in fact the background feature (similar to that seen as a “hump” in Fig. 1(c)) found in our calculations may enable one to bring the two experiments in closer agreement.

At  $\omega = \pm 22$  meV, the calculated (110) structures, which correspond to forward (intranodal) scattering, are stronger than the (100) structures. Preliminary numerical calculations suggest that scattering from order parameter fluctuations may contribute to  $\mathbf{q}_1$ -type peaks, leading to the interesting question of how the interplay of disorder and order parameter fluctuations manifests itself in the FTDOS. It is a general feature of our calculations at higher energies that the  $\mathbf{q}_1$  peaks are weaker than observed in experiments, and a tendency to stripe formation along the Cu-O bonds, as proposed in [7, 8, 9], could possibly enhance the weight near the  $\mathbf{q}_1$  peaks. However, stripe formation is difficult to reconcile with the dispersal of the  $\mathbf{q}_1$  peak[10, 11].

*Conclusions.* Existing analyses of recent STM measurements of the FTDOS have established the fundamental point that the structures in the FTDOS are dispersive and therefore likely represent interference of disordered quasiparticle wavefunctions. We have argued, using a combination of analytical and numerical approaches, that previous weak-scattering analyses are inadequate to explain the details of the FTDOS, however. In previous works it was expected that sharp “octet” peaks would broaden into the observed structures due to impurity scattering; here we have shown that these peaks are lost in the noise created by the interference of many impurities, rather than broadened. Our work suggests that the dispersing features observed may not correspond directly to the predicted sharp peaks at all, but rather to dispersive background structures which have hitherto been ignored. We show that the simplest “realistic” disorder model of unitary impurities and a smooth random potential explains many features of the FTDOS at lower energies, but at higher energies the comparison is worse, probably reflecting our lack of knowledge of the true smooth component of the disorder, including the local order parameter fluctuations neglected here. Further refining of these comparisons will be extremely important in understanding the origin of the nanoscale inhomogeneities observed in STM experiments.

*Acknowledgements.* The authors would like to thank D.J. Scalapino, R. Sedgewick, J.C. Davis and K. McElroy for several pivotal discussions. WAA would like to acknowledge Research Corporation Grant CC5543.

---

[1] Ali Yazdani, C. M. Howald, C. P. Lutz, A. Kapitulnik, and D. M. Eigler, Phys. Rev. Lett. **83**, 176 (1999).

[2] E.W. Hudson, S.H. Pan, A.K. Gupta, K-W Ng, and J.C.

- Davis, *Science* **285**, 88 (1999)
- [3] S. H. Pan, E. W. Hudson, K. M. Lang, H. Eisaki, S. Uchida, J. C. Davis, *Nature*, 403, 746 (2000).
  - [4] T. Cren *et al.*, *Phys. Rev. Lett.* **84**, 147 (2000).
  - [5] S.-H. Pan *et al.*, *Nature* **413**, 282 (2001).
  - [6] K.M. Lang, V. Madhavan, J. E. Hoffman, E. W. Hudson, H. Eisaki, S. Uchida and J.C. Davis, *Nature* **415**, 412 (2002).
  - [7] C. Howald, P. Fournier, and A. Kapitulnik, *Phys. Rev. B* **64**, 100504 (2001).
  - [8] C. Howald, H. Eisaki, N. Kaneko, A. Kapitulnik, cond-mat/0201546
  - [9] C. Howald, H. Eisaki, N. Kaneko, M. Greven, A. Kapitulnik, cond-mat/0208442.
  - [10] J. E. Hoffman *et al.*, *Science* **295**, 466 (2002).
  - [11] McElroy *et al.* *Nature* (2003).
  - [12] J. M. Byers, M. E. Flatté, and D. J. Scalapino, *Phys. Rev. Lett.* **71**, 3363 (1993).
  - [13] A. V. Balatsky, M. I. Salkola, and A. Rosengren, *Phys. Rev. B* **51** 15 547 (1995).
  - [14] J. Friedel, *Phil. Mag* 43, 153 (1952).
  - [15] Degang Zhang and C. S. Ting, cond-mat/0209318.
  - [16] Qiang-Hua Wang and Dung-Hai Lee, *Phys. Rev. B* **67**, 020511 (2003).
  - [17] B. M. Anderson and P. Hedegard, cond-mat/0301225 .
  - [18] D. Zhang and C.S. Ting, cond-mat/0304176.
  - [19] L. Capriotti, D.J. Scalapino, and R. D. Sedgewick, preprint 2003.
  - [20] M. R. Norman, M. Randeria, H. Ding, and J. C. Campuzano, *Phys. Rev. B* **52**, 615 (1995).
  - [21] T. Pereg-Barnea and M. Franz cond-mat/0306712.
  - [22] J.X. Zhu, C.S. Ting, and C.R. Hu, *Phys. Rev. B* **62**, 6027 (2000).
  - [23] I. Martin, A. V. Balatsky, and J. Zaanen, *Phys. Rev. Lett* **88**, 097003 (2002).
  - [24] The 1-impurity FTDOS is somewhat different than in Ref. [16] because of the larger value of  $\Delta_0$  used here.
  - [25] See e.g. A. M. Martin and James F. Annett, *Phys. Rev. B* **57** 8709 (1998); Roger Haydock and Ronald L. Te, *Phys. Rev. B* **49**, 10845 (1994).
  - [26] P. J. Hirschfeld, Lingyin Zhu, and W. A. Atkinson, unpublished.
  - [27] J. C. Davis and K. McElroy, private communication.